Structure of the I_1 early intermediate of photoactive yellow protein by FTIR spectroscopy

Ronald Brudler[1], Robin Rammelsberg[2], Tammy T. Woo[1], Elizabeth D. Getzoff[1] and Klaus Gerwert[2]

To understand how proteins translate the energy of sunlight into defined conformational changes, we have measured the photocycle reactions of photoactive yellow protein (PYP) using time-resolved step scan Fourier transform infrared (FTIR) spectroscopy. Global fit analysis yielded the same apparent time constants for the reactions of the chromophore, the protonation changes of protein side chains and the protein backbone motions, indicating that the light cycle reactions are synchronized. Changes in absorbance indicate that there are at least four intermediates (I_1, I_1', I_2, I_2'). In the intermediate I_1, the dark-state hydrogen bond from Glu 46 to the aromatic ring of the *p*-hydroxycinnamoyl chromophore is preserved, implying that the chromophore undergoes *trans* to *cis* isomerization by flipping, not the aromatic ring, but the thioester linkage with the protein. This excludes an I_1 structural model proposed on the basis of time resolved Laue crystallography, but does agree with the cryotrapped structure of an I_1 precursor.

Understanding protein function at the atomic level is a major challenge for biophysics today and requires the combined efforts of structural and functional methods. We use photoactive yellow protein (PYP; Fig. 1) as a model system to understand in atomic detail how a chromophore and a protein interact to sense light and send a biological signal. PYP is a cytoplasmic blue-light receptor from purple bacteria[1–3], in which it appears to serve as the sensor for negative phototaxis[4]. PYP's small size (14 kDa)[5,6], simple chromophore[6,7], high stability[8], simple self-contained light cycle[5,9–11], and the ease with which high quality crystals can be generated[12] make it an attractive target for studying the molecular basis of light detection, intracellular signaling and dynamic structural changes in proteins.

Upon absorption of a photon by its covalently attached *p*-hydroxycinnamoyl chromophore, PYP undergoes a cyclic sequence of reactions. The ground state P (λ_{max} of 446 nm) is converted into the intermediate I_1 (λ_{max} of 465 nm) in ~3 ns. I_1 (also called pR or PYP_L in the literature) is then converted into the long lived blue-shifted intermediate I_2 (λ_{max} of 350 nm; also called pB or PYP_M), which returns to the ground state P. No consensus exists for the number of time constants of these reactions. Consequently for the photocycle model, the $I_1 \rightarrow I_2$ and $I_2 \rightarrow P$ transitions have been described either by monophasic decays with time constants of 200 μs and 140 ms, respectively[11], or by two biexponential decays with time constants of 250 μs and 1.2 ms (decay of I_1) and 150 ms and 2.0 s (decay of I_2)[9]. High resolution structures of PYP in the ground state[13,14], the intermediate I_1[15], a cryotrapped intermediate preceeding I_1[16] and the intermediate I_2[17] are available. But the models for the early photocycle intermediates and chromophore isomerization differ substantially[15,16], and spectroscopic and thermodynamic data for PYP in solution[18–20] point to a larger structural change for I_2 than that found in the crystal[17].

Fourier transform infrared (FTIR) and Raman spectroscopy are powerful methods for studying the reaction mechanisms of proteins because they detect vibrational frequencies and intensities of individual functional groups with high sensitivity and time resolution, and yield information about structural changes during protein function[21–23]. Raman spectroscopy selectively detects chromophore vibrations, while infrared spectra contain contributions from all the protein components. The complexity of infrared spectra, however, can be overcome by calculating the difference between the ground state and an activated state of a protein. Difference spectra eliminate the background absorption of the protein and show exclusively those groups that undergo changes during the reaction. These groups can be assigned by mutagenic or isotopic substitutions, and their reac-

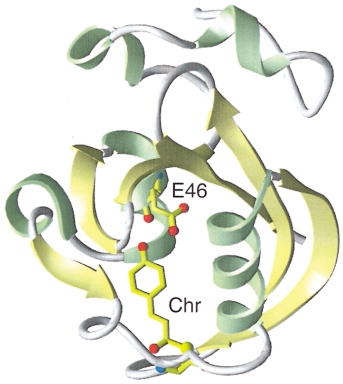

Fig. 1 Overall view of the PYP ground state structure. The 125-residue polypeptide chain is shown as a ribbon model with β-sheets, α-helices, and connecting loops in yellow, green, and gray, respectively. In the active site, the anionic chromophore (Chr) and protonated Glu 46, which are discussed in the text, are shown in yellow (red spheres oxygens, blue spheres nitrogens, yellow sphere sulfur). The *p*-hydroxycinnamoyl chromophore is covalently linked by a thioester to the only Cys of the protein and hydrogen bonded at its phenolate oxygen by the side chain of Glu 46.

[1]Department of Molecular Biology and Skaggs Institute for Chemical Biology, The Scripps Research Institute, La Jolla, California 92037, USA. [2]Lehrstuhl für Biophysik, Ruhr-Universität Bochum, D-44780 Bochum, Germany.

Correspondence should be addressed to R.B. *email: rbrudler@scripps.edu* or K.G. *email: gerwert@bph.ruhr-uni-bochum.de*

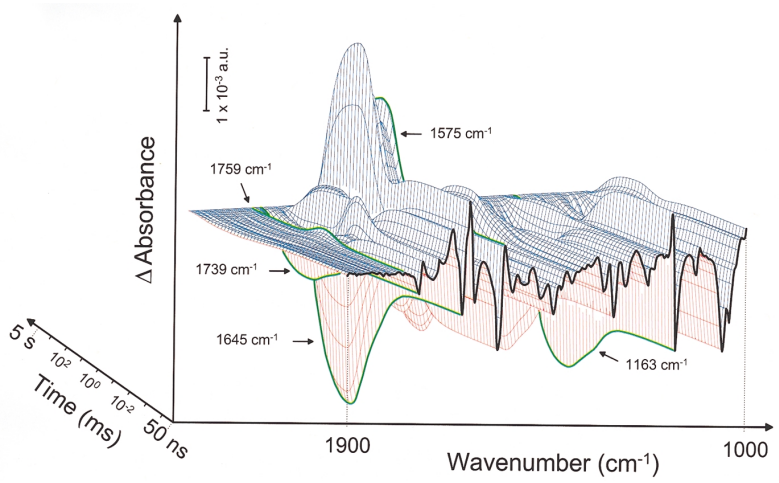

Fig. 2 Three-dimensional representation of the fitted infrared absorbance changes of PYP. The absorbance changes were fit with the global fit program (see Methods) and are shown as a function of wavenumber (1900–1000 cm^{-1}) and time on a logarithmic scale (50 ns to 5 s). The first difference spectrum, recorded 50 ns after laser flash excitation, is highlighted in black and represents an I_1 - P difference spectrum (compare with Fig. 3). The subsequent difference spectra show the reaction from I_1 *via* I_2 back to the ground state P (compare with Fig. 4). The kinetic traces at the labeled wavenumbers (green) are discussed in the text and shown together with the raw data in Fig. 5, where the quality of the global fit can be judged.

tions can be followed in real time. Here, we report the first time-resolved FTIR study on PYP. The results allow us to derive a structural model for the intermediate I_1 and to propose an extended photocycle model with two additional intermediates, I_1' and I_2'.

A three-dimensional representation of the light induced infrared absorbance changes during the photocycle of PYP, measured simultaneously from 1900–1000 cm^{-1}, is shown in Fig. 2. The time resolution of 30 ns allowed monitoring of the light cycle reactions starting from the intermediate I_1 and proceeding *via* the intermediate I_2 back to the ground state P. Global fit analysis of the absorbance changes yielded four apparent time constants, τ_1 = 113 µs, τ_2 = 1.5 ms, τ_3 = 189 ms, and τ_4 = 583 ms. Fits with two or three exponentials did not describe the data satisfactorily. Below, we first describe the difference spectra corresponding to single photocycle intermediates and then analyze the kinetics at specific wavenumbers.

FTIR difference spectra of photocycle intermediates

The I_1 - P FTIR difference spectrum, recorded 1 µs after the laser flash (Fig. 3), shows the light induced absorbance changes between the ground state P (negative bands) and early intermediate I_1 (positive bands). Most negative peaks (1560, 1530, 1436, 1302, 1162, 1057, 1042 and 982 cm^{-1}) align with the chromophore modes seen in the PYP ground state by FT Raman spectroscopy (Fig. 3). We conclude from this and the relatively small size of the amide I difference band at 1643/1626 cm^{-1}, which represents the C=O stretching vibrations of the protein backbone amide groups, that the P → I_1 reaction is mainly characterized by chromophore isomerization and that the protein cannot fully respond to chromophore isomerization on the ns time scale.

To further characterize the P → I_1 transition, the bands at 1739 and 1730 cm^{-1} were assigned with the aid of the PYP E46Q mutant (Fig. 3, inset). Deprotonation (protonation) of a carboxyl (carboxylate) group is indicated by a negative (positive) band in the region of the carbonyl stretching vibrations between 1780 and 1700 cm^{-1}; the COO^- carboxylate group absorbs at lower frequencies and is difficult to assign due to extensive overlap with other protein and chromophore bands. The negative band at 1739 cm^{-1} and positive band at 1730 cm^{-1} could be caused by two different carboxylic acids that become deprotonated and protonated, respectively, during the P → I_1 transition. The similar shape and integrated intensity of the two bands at 1739 and 1730 cm^{-1} and the absence of both bands in the I_1 - P difference spectrum of the E46Q mutant (Fig. 3, inset) indicate, however, that both bands must be assigned to Glu 46. The shift of 9 cm^{-1} from 1739 to 1730 cm^{-1} implies[24] that the carboxyl group of Glu 46 remains protonated in I_1 and strengthens its hydrogen bond to the chromophore's phenolate oxygen.

A similar difference band (at 1740/1732 cm^{-1}), observed in a static infrared difference spectrum of wild type PYP collected at 80 K with illumination at 410 nm, was tentatively assigned to

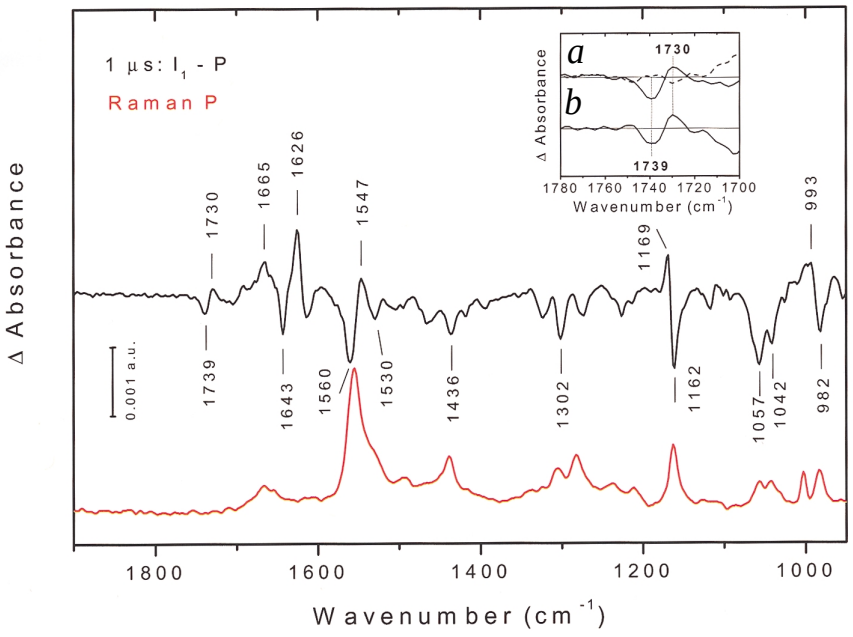

Fig. 3 I_1 – P FTIR difference spectrum and FT Raman spectrum of P. The I_1 – P FTIR difference spectrum for wild type PYP (black line, matches front curve in Fig. 2) was recorded 1 µs after light excitation and is compared to the FT Raman spectrum of the ground state P (red line). The inset shows: *a*, the enlarged I_1 – P FTIR difference spectrum in the region of the carbonyl stretching vibrations between 1780 and 1700 cm^{-1} for wild type PYP (solid line) and the PYP mutant E46Q (dashed line); and *b*, the double difference spectrum (wild type minus mutant). The straight lines in the inset are the zero lines.

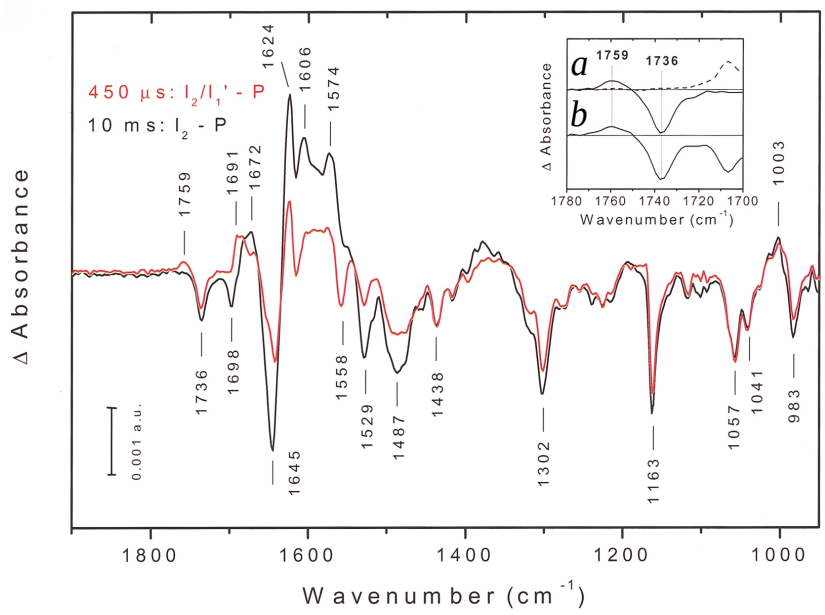

Fig. 4 I_2 – P and I_2/I_1' – P FTIR difference spectra. The I_2 – P (black line) and I_2/I_1' – P (red line) FTIR difference spectra were recorded 10 ms and 450 µs after light excitation, respectively. The inset shows: *a*, the I_2/I_1' – P difference spectrum between 1780 and 1700 cm^{-1} for wild type PYP (solid line) and the PYP mutant E46Q (dashed line); and *b*, the double difference spectrum between wild type and the mutant. The straight lines in the inset are the zero lines.

Glu 46 (ref. 25) on the basis of the ground state PYP crystal structure. At this temperature, however, photocycle intermediate I_1 (λ_{max} of 465 nm) is not formed. Instead, PYP exists as a steady state mixture of two different photoproducts[10,26], termed PYP_B (λ_{max} of 489 nm) and PYP_H (λ_{max} of 442 nm)[10], indicating that Glu 46 is protonated in these early intermediates as well.

The I_2 – P difference spectrum, recorded 10 ms after the laser flash (Fig. 4, black line), shows the absorbance changes between the ground state P (negative bands) and the intermediate I_2 (positive bands). The bands at 1529, 1438, 1302, 1163, 1057, 1041 and 983 cm^{-1} are identified as chromophore ground state vibrations by comparison with the FT Raman spectrum in Fig. 3. By comparison with the resonance Raman spectrum of the intermediate I_2[27], the strong positive bands at 1606 and 1574 cm^{-1} are assigned at least in part to coupled C–C and C=C stretching vibrations of the chromophore's aromatic ring and vinyl group and indicate that the chromophore is protonated and in the *cis* configuration in I_2. The largest signal in the I_2 – P difference spectrum, however, is observed for the amide I band at 1645/1624 cm^{-1}. The integrated intensity of this signal between 1650 and 1615 cm^{-1} is ~2.5% of PYP's backbone absorption, in agreement with Hoff *et al.*[20]. This value is larger than for other photoreceptors, for example membrane proteins like the photosynthetic reaction center and bacteriorhodopsin[21] or a cytoplasmic protein like phytochrome[28], and points to a larger movement of PYP's protein backbone in the $I_1 \rightarrow I_2$ transition.

In the time resolved I_2 – P difference spectrum of the PYP E46Q mutant (not shown), the negative band at 1736 cm^{-1} is missing and was, therefore, assigned to Glu 46. A corresponding assignment was performed using the E46Q mutant in a static I_2 – P difference spectrum recorded at -40 °C with irradiation >450 nm[29]. The negative band indicates that Glu 46 becomes deprotonated upon formation of I_2.

The difference spectrum 450 µs after the laser flash (Fig. 4, red line) closely resembles the I_2 – P difference spectrum recorded at 10 ms (Fig. 4, black line), especially below 1450 cm^{-1}, but has an additional positive band at 1759 cm^{-1}. This band shifts by -10 cm^{-1} in D_2O (not shown), as expected for a carboxylic acid, and disappears in the E46Q mutant (Fig. 4, inset). Therefore, the band at 1759 cm^{-1}, like the band at 1736 cm^{-1} (see above), is assigned to Glu 46. The 23 cm^{-1} shift to higher frequencies shows[24] that Glu 46 moves into a hydrophobic environment but stays protonated. This is in agreement with the unique location of Glu 46 in PYP; of 20 carboxyl groups (12 Asp, 7 Glu and the C-terminus) all are solvent exposed except for Glu 46, which is buried[13].

Infrared kinetics at specific wavenumbers

Vibrations that characterize changes of specific functional groups during the photocycle were selected for further kinetic analysis (see below). The C=O stretching vibrations of Glu 46 were followed at 1759 cm^{-1} (Fig. 5*a*) and 1739 cm^{-1} (Fig. 5*b*). The coupled C–C/C=C stretching vibration at 1575 cm^{-1} (Fig. 5*c*) monitors the protonated *cis*-chromophore[27]. Because it overlaps with protein contributions, the chromophore kinetics were also followed at 1163 cm^{-1} (Fig. 5*c*), where overlaps do not occur. The chromophore protonates with time constants τ_1 (113 µs) and τ_2 (1.5 ms), and deprotonates and reisomerizes to the *trans* configuration with τ_3 (189 ms) and τ_4 (583 ms).

Movements of the protein backbone were followed by absorbance changes of the amide I difference signal at 1645/1624 cm^{-1} (Fig. 5*d*). A significant structural change that appears with time constants τ_1 and τ_2 returns to the ground state conformation with τ_3 and τ_4. Above 1770 cm^{-1} a broad continuum absorbance change (ΔA ~5×10^{-5} absorbance units) was observed (Fig. 2), decreasing with τ_1 and τ_2 and increasing with τ_3 and τ_4. The continuum band describes the polarizability changes of a delocalized proton within a hydrogen bonded network[30].

Mechanism of chromophore isomerization

Analysis of the time resolved FTIR measurement allowed the development of a structural model for the chromophore isomerization reaction. In the ground state P, the anionic chromophore is buried in a hydrophobic core and tethered to the protein by a network of hydrogen bonds[13] (Fig. 6). The phenolate oxygen of the chromophore hydrogen bonds with the hydroxyl group of Tyr 42 and the protonated carboxyl group of Glu 46. The side chain oxygen of Thr 50 forms a bifurcated hydrogen bond with the hydroxyl group of Tyr 42 and the main chain carbonyl oxygen of Glu 46. In addition, the guanidinium group of Arg 52 forms hydrogen bonds with the main chain oxygens of Thr 50 and Tyr 98 (Fig. 6). The tight packing of the protein core strongly constrains chromophore mobility and limits the possible mechanisms of *trans* to *cis* isomerization, which takes place on a fs time scale after light absorption[31]. The time resolved FTIR data for the intermediate I_1, which forms in ~3 ns, show that the carboxyl group of Glu 46 remains protonated, and its hydrogen bond to the chromophore's phenolate oxygen is preserved and strengthened (Fig. 3). The preservation of this ground state

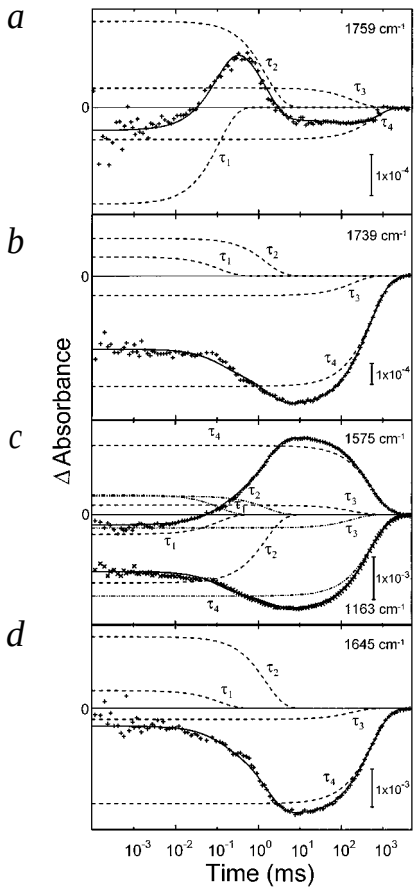

Fig. 5 Infrared kinetics at specific wavenumbers. ***a***, C=O stretching vibration of Glu 46 at 1759 cm^{-1}; ***b***, C=O stretching vibration of Glu 46 at 1739 cm^{-1}. The kinetic trace starts below the zero line because the small movement of Glu 46 during the P → I_1 transition is not time resolved. ***c***, Chromophore vibrations at 1575 cm^{-1} and 1163 cm^{-1}. ***d***, C=O stretching vibrations of the protein backbone amide groups at 1645 cm^{-1} (amide I band). The kinetic trace starts below the zero line because a smaller change of the amide I absorption has already occurred in the P → I_1 transition. The fits (solid line) are composed of the sum of single exponentials (dashed lines), as revealed by global fit analysis.

hydrogen bond implies that the chromophore's aromatic head group has not moved significantly, which is only possible if the isomerization takes place by flipping not the aromatic ring, but the thioester linkage between the chromophore and the protein. Flipping of the thioester linkage by co-isomerization around the chromophore's C=C vinyl double bond and the C–S single bond requires only minor displacements (<4 Å) of the chromophore's carbonyl oxygen and sulfur atom, whereas isomerization around the vinyl double bond alone requires substantial displacement of the chromophore's aromatic ring[16,25].

Structure of the I_1 intermediate

The time resolved FTIR data at room temperature preclude the structure of PYP photocycle intermediate I_1 proposed on the basis of time resolved Laue crystallography[15]. In this model, in-plane rotation of the aromatic chromophore ring increases the distance between the Glu 46 side chain oxygen and the phenolate oxygen of the chromophore to 4.6 Å, breaking this hydrogen bond (Fig. 6). We assume that the low occupancy of the I_1 intermediate in the crystal (15%) in combination with a relatively low resolution (1.9 Å) did not allow an appropriate crystallographic refinement of the structure of a photocycle intermediate that does not show canonical geometrical parameters for the chromophore. This view is supported by inspection of the difference Fourier map shown in Fig. 3 of ref. 15. The few regions of positive and negative electron density (at the 2.6 σ level) near the chromophore ring and the isomerizable double bond do not support the chromophore fit. The most prominent positive electron density feature (+5.0 σ) close to the chromophore's carbonyl group (denoted L)[15] was ascribed to a repositioning of the chromophore's vinyl carbon atoms and was not fit with the carbonyl group of the chromophore. Thus, the model does not show a flipping of the thioester linkage required by the FTIR data. It seems more likely that electron density L represents the flipped carbonyl group of the chromophore after isomerization.

The FTIR results are, however, in agreement with the 0.85 Å resolution X-ray structure of an early PYP photocycle intermediate trapped by cooling the crystal below -100 °C and subsequent light activation[16]. Under these conditions, a blue-shifted precursor of the I_1 intermediate accumulates. The chromophore of this intermediate has undergone *trans* to *cis* isomerization by flipping of the thioester linkage (Fig. 6). Correspondingly, the largest atomic movements are found for the chromophore's carbonyl oxygen (3.4 Å) and sulfur atom (1.4 Å). The chromophore's aromatic ring moves only slightly due to the small lengthwise contraction of the chromophore of 0.4 Å upon isomerization. The direct hydrogen bond donors to the chromophore, Tyr 42 (largest atomic shift 0.31 Å) and Glu 46 (0.13 Å shift), follow this movement, but the hydrogen bonds between these residues and the chromophore's phenolic oxygen are preserved, in agreement with the FTIR data. In this cryotrapped intermediate, the chromophore had barely crossed the *trans* to *cis* transition point (torsion angle -80° around the vinyl double bond), and it was concluded that formation of I_1 mainly involves the continuation of the rotation around this bond to form a fully *cis* configuration[16]. This is corroborated by the FTIR data, which indicate in addition that the hydrogen bond between the protonated carboxylate of Glu 46 and the phenolate oxygen of the chromophore (2.69 Å in the ground state, 2.77 Å in the early photocycle intermediate) becomes stronger in the I_1 intermediate.

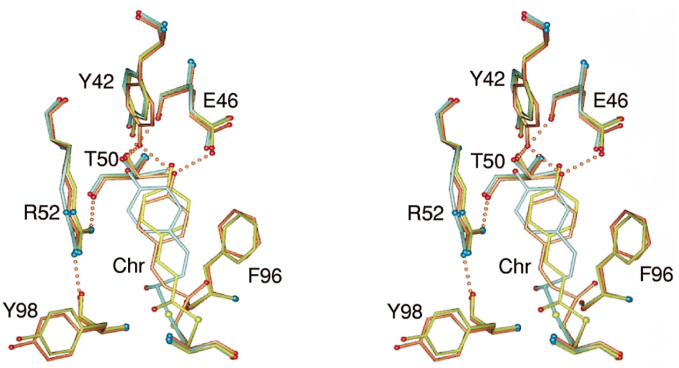

Fig. 6 Stereo view of PYP's active site. Shown are the models for the ground state[13] (yellow; PDB code 2PHY) and early photocycle intermediates trapped by time resolved Laue crystallography 1 ns after light excitation[15] (green; PDB code 2PYR) or cryogenic cooling[16] (red; PDB code 3PYP). The hydrogen bonds of the PYP ground state are preserved in the cryotrapped intermediate and are indicated by red dots. The atomic positions for Phe 96 and Tyr 98 were not refined in ref. 15. Chr, chromophore.

Experimentally addressing functionally important conformational changes that occur in sub-ms processes is extremely challenging. Although in principle Laue X-ray diffraction experiments can be performed on ns or faster time scales, the partial occupancy often arising from rapid activation, and the reduced spacial resolution and signal-to-noise ratio resulting from the extremely short data collection times all degrade the ability to distinguish the relatively small conformational changes that are allowed on these time scales. The evident difficulties in interpretation of difference features from Laue data in well-diffracting systems such as PYP[15] and myoglobin[32] explain conflicts with high resolution freeze-trapped structures of these systems[16,33]. Structural characterization by FTIR spectroscopy, with its high sensitivity to minor changes in bond lengths, bond angles, protonation, and hydrogen bonding, and its applicability to liquid samples, is a powerful complementary technique to well-established crystallographic approaches.

Photocycle model

Global fit analysis yielded the same four time constants (τ_1 = 113 μs, τ_2 = 1.5 ms, τ_3 = 189 ms, τ_4 = 583 ms) for the chromophore reactions, side chain protonation changes and protein backbone motion (Fig. 5). We conclude that all the reactions are synchronized and that there are no independent cycles for different parts of the protein. Similar time constants were found in the UV/visible spectra range[9] (τ_1 = 250 μs, τ_2 = 1.2 ms, τ_3 = 150 ms, and τ_4 = 2 s). Small deviations may have been caused by different measuring conditions (20 mM Hepes, pH 7.0, 22 °C *versus* 10 mM Tris-HCl, pH 7.5, 19 °C in ref. 9).

The observed apparent time constants can be explained in principle by a linear (single pathway) reaction scheme or parallel photocycles. To discern between these possibilities, the interpretation of the band at 1759 cm^{-1} is crucial. Its disappearance in the E46Q mutant and the unique location of Glu 46 inside PYP show that this band is due to Glu 46. In a linear reaction scheme, the rise of the difference band at 1759/1736 cm^{-1} (Fig. 4, red line) with τ_1 (113 μs) is interpreted as the movement of Glu 46 into a hydrophobic environment, and deprotonation of Glu 46 occurs with τ_2 (1.5 ms) (Fig. 5*a*,*b*). The very different integrated intensities of the bands at 1759 cm^{-1} and 1736 cm^{-1} (ratio ~1:4), however, argue against this scheme and favor a parallel photocycle model. In such a model, starting from the intermediate I_1 two events occur in parallel with time constant τ_1 (113 μs): movement of Glu 46 into a hydrophobic environment in about one quarter of the PYP molecules (formation of I_1'), as indicated by the rise and intensity of the band at 1759 cm^{-1} (Fig. 5*a*); and deprotonation of Glu 46 in the main PYP population (formation of I_2), as monitored at 1739 cm^{-1} (Fig. 5*b*). The rate τ_2 (1.5 ms) involves further deprotonation of Glu 46, in the minority population, as indicated by the disappearance of the band at 1759 cm^{-1} and the absorbance increase at 1739 cm^{-1} (Figs 4, 5*a*,*b*). The reactions described by τ_1 and especially τ_2 also involve a significant movement of the protein backbone as monitored at 1645 cm^{-1} (Figs 2, 5*d*).

Glu 46 deprotonates (τ_1 = 113 μs and τ_2 = 1.5 ms) and reprotonates (τ_3 = 189 ms and τ_4 = 583 ms) with the same time constants as the chromophore (Fig. 5*a*–*c*). Therefore, Glu 46 is most probably the proton donor to the chromophore. Alternatively, the chromophore could be protonated by a water molecule that could enter the active site upon formation of I_2 and I_1'. This possibility cannot be ruled out, especially if proton transfer from the water molecule to the chromophore were much faster than proton transfer from Glu 46 to this water molecule.

Satisfactory fitting of the absorbance changes in the infrared region requires two slow time constants (τ_3 = 189 ms, τ_4 = 583 ms), indicating the formation of the intermediate I_2' following I_2. The intermediates I_2 and I_2', however, follow too closely in time to define specific differences between them. Further experiments are necessary to resolve the reactions and their order, leading to reformation of the PYP ground state, including chromophore re-isomerization and deprotonation, protein refolding, and protonation of Glu 46.

The FTIR data reported here enable us to extend the present photocycle model by two new intermediates (I_1', I_2') and establish the structural characteristics of the I_1 intermediate. Our results complement other biophysical studies[16,25] and demonstrate consistently that PYP's early intermediates (up to and including I_1) store light energy in the *cis* isomer of the anionic *p*-hydroxycinnamoyl chromophore by flipping its thioester linkage, while preserving the dark-state hydrogen bond with the protonated Glu 46.

Methods

Sample preparation. Expression of recombinant wild type PYP from *Ectothiorhodospira halophila* and of the PYP mutant E46Q in *Escherichia coli*, chromophore attachment, and protein purification were performed as described[34]. For the FTIR experiments, 360 μg wild type or E46Q PYP in 20 mM Hepes, pH 7.0, was pipetted on the center of a CaF_2 window with a 2.5 μm thick teflon spacer, dried in a gentle stream of nitrogen, and resolubilized with 1 μl 20 mM Hepes, pH 7.0. The sample was covered with a second CaF_2 window, sealed with apiezone grease and thermostabilized at 22 °C in the spectrometer. For the FT Raman experiment, 4 μl of 40 mg ml^{-1} PYP in 20 mM Hepes buffer, pH 7.0, were pipetted into a quartz capillary and thermostabilized at 22 °C in a home built sample holder[35] in the spectrometer.

FT Raman spectroscopy. FT Raman spectra were recorded with an FRA 106 FT Raman module connected to an IFS 88 FTIR spectrometer (Bruker) as described[35]. Sixty spectra, each consisting of 200 scans, were averaged to improve the signal-to-noise ratio.

Step scan FTIR difference spectroscopy. Time resolved step scan FTIR spectroscopy was performed on a vacuum FTIR spectrometer (Bruker, IFS 66v) with a globar infrared source, KBr beam splitter and a photovoltaic HgCdTe detector (Kollmar Technologies, KVMP11-1-J2) as described[36]. Spectra were recorded with 30 ns time resolution and a spectral resolution of 6.0 cm^{-1} between 1974 and 900 cm^{-1}. The sample was excited with an excimer-pumped dye laser system (Lambda Physik, LPX 300, FL 105) at 396 nm. The laser flashes were separated by 4 s. A total of 99 measurements was averaged in order to improve the signal-to-noise ratio. Between the measurements, kinetics at 460 nm were recorded on the same sample and compared with the kinetics of PYP in solution to control the activity of the sample. The reconstruction of the interferograms and the computation of the difference spectra were carried out with the OPUS software from Bruker.

Global fit data analysis. The absorbance changes ΔA at all wavenumbers ν_i were fitted with the sums of n_r exponentials with apparent time constants τ_n and amplitudes a_n, where τ_n is the same for all i: $\Delta A(\nu_i,t) = \Sigma a_n(\nu_i)e^{-t/\tau n}$. A detailed description of the global fit procedure is given in ref. 37.

Acknowledgments

This work was supported by grants from the NIH to E.D.G. and the DFG to K.G. R.B. gratefully acknowledges a fellowship from the DFG.

Received 12 September, 2000; accepted 5 January, 2001.

1. Meyer, T.E. Isolation and characterization of soluble cytochromes, ferredoxins and other chromophoric proteins from the halophilic phototrophic bacterium. *Ectothiorhodospira halophila*. *Biochim. Biophys. Acta* **806**, 175–183 (1985).
2. Kort, R. *et al.* The xanthopsins; a new family of eubacterial blue-light photoreceptors. *EMBO J.* **15**, 3209–3218 (1996).
3. Jiang, Z.Y. *et al.* Bacterial photoreceptor with similarity to photoactive yellow protein and plant phytochromes. *Science* **285**, 406–409 (1999).
4. Sprenger, W.W., Hoff, W.D., Armitage, J.P. & Hellingwerf, K.J. The eubacterium *Ectothiorhodospira halophila* is negatively phototactic, with a wavelength dependence that fits the absorption spectrum of the photoactive yellow protein. *J. Bacteriol.* **175**, 3096–3104 (1993).
5. Meyer, T.E., Yakali, E., Cusanovich, M.A. & Tollin, G. Properties of a water-soluble, yellow protein isolated from a halophilic phototrophic bacterium that has photochemical activity analogous to sensory rhodopsin. *Biochemistry* **26**, 418–423 (1987).
6. Baca, M. *et al.* Complete chemical structure of photoactive yellow protein: novel thioester-linked 4-hydroxycinnamyl chromophore and photocycle chemistry. *Biochemistry* **33**, 14369–14377 (1994).
7. Hoff, W.D. *et al.* Thiol ester-linked p-coumaric acid as a new photoactive prosthetic group in a protein with rhodopsin-like photochemistry. *Biochemistry* **33**, 13959–13962 (1994).
8. Meyer, T.E., Tollin, G., Hazzard, J.H. & Cusanovich, M.A. Photoactive yellow protein from the purple phototrophic bacterium, *Ectothiorhodospira halophila*. Quantum yield of photobleaching and effects of temperature, alcohols, glycerol, and sucrose on kinetics of photobleaching and recovery. *Biophys. J.* **56**, 559–564 (1989).
9. Hoff, W.D. *et al.* Measurement and global analysis of the absorbance changes in the photocycle of the photoactive yellow protein from *Ectothiorhodospira halophila*. *Biophys. J.* **67**, 1691–1705 (1994).
10. Imamoto, Y., Kataoka, M. & Tokunaga, F. Photoreaction cycle of photoactive yellow protein from *Ectothiorhodospira halophila* studied by low-temperature spectroscopy. *Biochemistry* **35**, 14047–14053 (1996).
11. Ujj, L. *et al.* New photocycle intermediates in the photoactive yellow protein from *Ectothiorhodospira halophila*; picosecond transient absorption spectroscopy**.** *Biophys. J.* **75**, 406–412 (1998).
12. McRee, D.E., Meyer, T.E., Cusanovich, M.A., Parge, H.E. & Getzoff, E.D. Crystallographic characterization of a photoactive yellow protein with photochemistry similar to sensory rhodopsin. *J. Biol. Chem.* **261**, 13850–13851 (1986).
13. Borgstahl, G.E.O., Williams, D.R. & Getzoff, E.D. 1.4 Å structure of photoactive yellow protein, a cytosolic photoreceptor: unusual fold, active site, and chromophore. *Biochemistry* **34**, 6278–6287 (1995).
14. Düx, P. *et al.* Solution structure and backbone dynamics of the photoactive yellow protein. *Biochemistry* **37**, 12689–12699 (1998).
15. Perman, B. *et al.* Energy transduction on the nanosecond time scale: early structural events in a xanthopsin photocycle. *Science* **279**, 1946–1950 (1998).
16. Genick, U.K., Soltis, S.M., Kuhn, P., Canestrelli, I.L. & Getzoff, E.D. Structure at 0.85 Å resolution of an early protein photocycle intermediate. *Nature* **392**, 206–209 (1998).
17. Genick, U.K. *et al.* Structure of a photocycle intermediate by millisecond time-resolved crystallography. *Science* **275**, 1471–1475 (1997).
18. van Brederode, M.E., Hoff, W.D., van Stokkum, I.H.M., Groot, M.L. & Hellingwerf, K.J. Protein folding thermodynamics applied to the photocycle of the photoactive yellow protein. *Biophys. J.* **71**, 365–380 (1996).
19. Rubinstenn, G. *et al.* Structural and dynamic changes of photoactive yellow protein during its photocycle in solution. *Nature Struct. Biol.* **5**, 568–570 (1998).
20. Hoff, W.D. *et al.* Global conformational changes upon receptor stimulation in photoactive yellow protein. *Biochemistry* **38**, 1009–1017 (1999).
21. Gerwert, K. Molecular reaction mechanisms of proteins as monitored by time-resolved FTIR spectroscopy. *Current Opin. Struct. Biol.* **3**, 769–773 (1993).
22. Siebert, F. Infrared spectroscopy applied to biochemical and biological problems. *Methods Enzymol.* **246**, 501–526 (1995).
23. Mathies, R.A. Biomolecular vibrational spectroscopy. *Methods Enzymol.* **246**, 377–389 (1995).
24. Gerwert, K., Hess, B., Soppa, J. & Oesterhelt, D. Role of aspartate-96 in proton translocation by bacteriorhodopsin. *Proc. Natl. Acad. Sci. USA* **86**, 4943–4947 (1989).
25. Xie, A., Hoff, W.D., Kroon, A.R. & Hellingwerf, K.J. Glu 46 donates a proton to the 4-hydroxycinnamate anion chromophore during the photocycle of photoactive yellow protein. *Biochemistry* **35**, 14671–14678 (1996).
26. Hoff, W.D., Kwa, S.L.S., van Grondelle, R. & Hellingwerf, K.J. Low temperature absorbance and fluorescence spectroscopy of the photoactive yellow protein from *Ectothiorhodospira halophila*. *Photochem. Photobiol.* **56**, 529–539 (1992).
27. Unno, M., Kumauchi, M., Sasaki, J., Tokunaga, F. & Yamauchi, S. Evidence for a protonated and *cis* configuration chromophore in the photobleached intermediate of photoactive yellow protein. *J. Am. Chem. Soc.* **122**, 4233–4234 (2000).
28. Foerstendorf, H., Mummert, E., Schafer, E., Scheer, H. & Siebert, F. Fourier-transform infrared spectroscopy of phytochrome: difference spectra of the intermediates of the photoreactions. *Biochemistry* **35**, 10793–10799 (1996).
29. Imamoto, Y. *et al.* Evidence for proton transfer from Glu-46 to the chromophore during the photocycle of photoactive yellow protein. *J. Biol. Chem.* **272**, 12905–12908 (1997).
30. Zundel, G. Proton polarizability and proton transfer processes in hydrogen bonds and cation polarizabilities of other cation bonds; their importance to understand molecular processes in electrochemistry and biology. *Trends Phys. Chem.* **3**, 129–156 (1992).
31. Devanathan, S. *et al.* Femtosecond spectroscopic observations of initial intermediates in the photocycle of the photoactive yellow protein from *Ectothiorhodospira halophila*. *Biophys. J.* **77**, 1017–1023 (1999).
32. Srajer, V. *et al.* Photolysis of the carbon monoxide complex of myoglobin; nanosecond time-resolved crystallography. *Science* **274**, 1726–1729 (1996).
33. Chu, K. *et al.* Structure of a ligand-binding intermediate in wild-type carbonmonoxy myoglobin. *Nature* **403**, 921–923 (2000).
34. Genick, U.K. *et al.* Active site mutants implicate key residues for control of color and light cycle kinetics of photoactive yellow protein. *Biochemistry* **36**, 8–14 (1997).
35. Brudler, R. *et al.* Coupling of hydrogen bonding to chromophore conformation and function in photoactive yellow protein. *Biochemistry* **39**, 13478–13486 (2000).
36. Rammelsberg, R., Hessling, B., Chorongiewski, H. & Gerwert, K. Molecular reaction mechanisms of proteins monitored by nanosecond step-scan FT-IR difference spectroscopy. *Appl. Spectrosc.* **51**, 558–562 (1997).
37. Hessling, B., Souvignier, G. & Gerwert, K. A model-independent approach to assigning bacteriorhodopsin's intramolecular reactions to photocycle intermediates. *Biophys. J.* **65**, 1929–1941 (1993).